Journal of Membrane Science 635 (2021) 119339

Contents lists available at ScienceDirect

Journal of Membrane Science

journal homepage: www.elsevier.com/locate/memsci

Long-term stable metal organic framework (MOF) based mixed matrix membranes for ultrafiltration

Muayad Al-Shaeli [a], Stefan J.D. Smith [a,b], Shanxue Jiang [c], Huanting Wang [a], Kaisong Zhang [d], Bradley P. Ladewig [c,e,*]

[a] Monash University, Department of Chemical Engineering, Clayton, VIC, 3800, Australia
[b] CSIRO, Manufacturing, Private Bag 33, Clayton South MDC, VIC 3169, Australia
[c] Barrer Centre, Department of Chemical Engineering, Imperial College London, Exhibition Road, London SW7 2AZ, United Kingdom
[d] Institute of Urban Environment, Chinese Academy of Sciences, No. 1799, Jimei Road, Xiamen 361021, China
[e] Institute for Micro Process Engineering (IMVT), Karlsruhe Institute of Technology, Hermann-von-Helmholtz-Platz 1, 76344 Eggenstein-Leopoldshafen, Germany

ARTICLE INFO

Keywords:
Polyethersulfone membrane
Anti-fouling
Phase inversion method
Mixed matrix membranes
UiO-66 and UiO-66-NH_2

ABSTRACT

In this study, novel mixed matrix membranes (MMMs) were synthesised by adding metal organic frameworks (MOFs) (UiO-66 and UiO-66-NH_2) to pristine and sulfonated polyethersulfone (PES). The differing synthetic method resulting in MMM where additives were grafted to the matrix polymer, or formed a natural interface, allowing the impact of these MMM features to be investigated. The composite membranes were characterised by FTIR, PXRD, water contact angle, porosity, pore size, etc. Membrane performance was investigated by water permeation flux, flux recovery ratio, fouling resistance and anti-fouling performance. The stability test was also conducted for all the prepared mixed matrix membranes. A higher reduction in the water contact angle was observed after adding both MOFs to the PES and sulfonated PES membranes compared to pristine PES membranes. An enhancement in membrane performance was observed by embedding the MOFs into PES membrane matrix, with flux increased remarkably (565 LMH for PES+UiO-66-NH_2 at 5% loading and 487.1 LMH for SPES-UiO-66(10% binding) while the BSA rejection was still kept at a high level. By adding the MOFs into PES matrix, the flux recovery ratio was increased greatly (more than 99% for most mixed matrix membranes). The mixed matrix membranes showed higher resistance to protein adsorption compared to pristine PES membranes. After immersing the membranes in water for 3 months, 6 months and 12 months, both MOFs were stable and retained their structure. This study indicates that UiO-66 and UiO-66-NH_2 are great candidates for designing long-term stable mixed matrix membranes (MMMs) for applications in water and wastewater treatment.

1. Introduction

With the increasing population around the world, the demand for clean and fresh water is increasing remarkably [1–3]. Membrane separation technology has been found as a quick response to the global demand of purified drinking water. The advantages like high filtration efficiency, simple operation, lower energy consumption, relatively low cost, and eco-friendliness lead to different applications of membrane separation technology [4–6]. As part of membrane separation processes, ultrafiltration (UF) is becoming a highly attractive technology due to their outstanding performance in removing dissolved organic macromolecules, suspended particles, and viruses [7,8]. An ideal UF membrane should have a high permeate flow rate, high solute rejection and high anti-fouling surface. To date, many polymeric materials such as polysulfone (PSF), polyethersulfone (PES), polyvinylidene fluoride (PVDF), and bromomethylated poly (phenylene oxide) (BPPO) are used to fabricate UF membranes [9–11]. However, the water flux and anti-fouling property of these polymer materials are quite low due to the hydrophobic nature which tend to cause membrane fouling. Membrane fouling affects negatively the performance of membrane by decreasing the flux, altering membrane selectivity, increasing operational cost and shortening membrane lifespan [12–14]. Thus, the modification of UF membranes for higher surface hydrophilicity is an effective way to overcome membrane fouling and improve the water flux [15–17].

In order to achieve a highly hydrophilic UF membrane, various approaches have been investigated including surface coating [18,19], blending with a hydrophilic polymer [20], grafting with hydrophilic

* Corresponding author at: Institute for Micro Process Engineering (IMVT), Karlsruhe Institute of Technology, Hermann-von-Helmholtz-Platz 1, 76344 Eggenstein-Leopoldshafen, Germany.
E-mail address: bradley.ladewig@kit.edu (B.P. Ladewig).

https://doi.org/10.1016/j.memsci.2021.119339
Received 17 December 2020; Received in revised form 12 March 2021; Accepted 5 April 2021
Available online 27 May 2021

monomers [21,22], incorporating of hydrophilic nanoparticles [23,24] and grafting with short-chain molecules [25]. Among these approaches, incorporating hydrophilic nanoparticles into the membrane matrix is a beneficial way to enhance the UF membrane performance. Numerous nanoparticles have been utilised to prepare mixed matrix membranes, including but not limited to titanium oxide [26], zirconium oxide [27], zinc oxide [28], carbon nanotubes [29], silicon dioxide [30], graphene oxide [31], and metal–organic frameworks (MOFs) [32]. Using these nanoparticles as additives would enhance the surface hydrophilicity, improve the pore formation, improve the interconnectivity of pores in the membranes and increase membrane performance in terms of permeability, rejection and anti-fouling properties [33].

MOFs are porous crystalline materials constructed from inorganic moieties connected by bridging organic clusters. They have been received a lot of attention among membrane researchers due to their extraordinary properties, such as high surface area, tunable and flexible pore structure, controlled porosity, higher crystallinity, high chemical and thermal stability, and low density. These properties make MOFs an ideal candidate for many industrial applications, including ultrafiltration membranes. MOFs offer a regular structure with uniform cavities, which can play a vital role to improve the hydrophilicity of the membranes by creating a solid interaction between polymer functional groups and MOFs [34,35]. Sorribas et al. [36] fabricated a polyamide nanocomposite membrane using different metal–organic frameworks via interfacial polymerisation. The obtained membranes showed an exceptional increase in the permeation flux after incorporating MIL-101 MOF, however, a slight loss in membrane selectivity. Low et al. [37] synthesised zeolitic imidazole framework-8 (ZIF-8) MOF with leaf-shaped structure and then entrapped it into PES membranes. The composite PES membranes showed improved membrane flux (75%) without significantly affecting the molecular weight cut-off. Li et al. [38] reported a preparation technique of PES nanofiltration membranes based on ZIF-8 via an interfacial method. The prepared PES membranes showed a significant improvement in rose bengal rejection (from 38.2% to 98.9%). The reduction in water permeation flux was corresponded to the hydrophobic character of ZIF-8. Shahid et al. [39] fabricated a hybrid membrane via in-situ growth of ZIF-8 in the polymer casting solution. The prepared membranes demonstrated a significant improvement in membrane performance, particularly for separation of CO_2/CH_4. Sun et al. [40] synthesised a hydrophilic hollow ZIF-8 MOF via surface functionalisation-assisted etching method using tannic acid. The synthesised MOF was introduced into PSF UF membranes via the phase inversion method. The hybrid membranes showed an enhancement in flux while keeping the rejection at a relatively high level. Gholami et al. [41] synthesised TMU-5 MOF as a filler and then incorporated it into PES UF membranes by blending it into the casting solution. The hybrid membranes showed higher anti-fouling properties, higher rejection, and higher water permeation flux when the concentration of MOF was low. These research studies showed the significant advantages of using MOF as nano-filler for application of water filtration. Nevertheless, it should be noted that most MOF-based mixed matrix membranes are employed for applications of gas separation due to the hydrophobic character of most of the MOFs, which could impact the water filtration performance of the prepared membranes. Although there have been studies on MOF-based membranes for water treatment, there are still several critical challenges, such as the development of effective technique to incorporate MOFs into membranes instead of physical blending [42]. Meanwhile, there were only a few studies focusing on the long-term stability of these membranes. This study aims to explore possible solutions to these challenges via different synthesis procedures (e.g., chemical grafting) and long-term stability studies.

In this study, two MOFs (UiO-66 and UiO-66-NH_2) were selected as the MOF candidates and PES was selected as the polymer. Chlorosulfonic acid is a strong sulfonating agent which is commonly used to sulfonate PES polymer due to its low cost, adaptability and simplicity, good film-forming capability, and ease of controlling the degree of functionalisation [43,44]. Furthermore, chlorosulfonic acid can not only react with UiO-66 and UiO-66-NH_2 due to presence of functional groups -NH_2 and -COOH, but also can function as a coupling agent to link PES polymer and MOF together [45,46]. Fig. 1 presents the mechanism of how the MOF can interact with SPES membranes.

2. Experimental section

2.1. Materials

Zirconium tetrachloride, terephthalic acid, benzoic acid, hydroxybenzoic acid, dimethylformamide (DMF), dimethylacetamide (DMAc), dichloromethane (anhydrous, ≥ 99.8%, contains 40–150 ppm amylene as stabiliser), polyethylene glycol (PEG, with MW of 20, 35, 100 and 200 kDa), and bovine serum albumin (BSA, 66 kDa, as foulant model) were provided by Sigma Aldrich, Australia. Amino-terephthalic acid and polyethersulfone (PES, Ultrason E6020P, 51 kDa) were purchased from BASF Co. Ltd., Germany. Sodium hydroxide pellets were purchased from Merck Millipore, Australia. The water used for the experiments was purified with a water purification system (Milli-Q integral water purification system, Merck Millipore Australia) with a resistivity of 18.2 MΩ/cm. Distilled water was obtained from a laboratory water distillation still (Lab glass Aqua III).

2.2. Synthesis of UiO-66 and UiO-66-NH2 MOFs

UiO-66 MOF was prepared as reported previously in the literature [47,48]. As shown in Figure S1, equimolar quantities (43 mmol) of terephthalic acid and zirconium tetrachloride were reacted in the existence of a large excess of benzoic acid (684 mmol) in a mixture of solvent DMF (1650 mL) and water (83 mL). The solid product was sequentially washed with methanol and DMF before being dried in vacuum oven at 120 °C for 24 h. UiO-66-NH_2 MOF was prepared as reported previously in the literature [49]. As shown in Figure S1, equimolar quantities (25 mmol) of aminoterephthalic acid and zirconium tetrachloride were mixed with 25 mL concentrated HCl (32% concentration) and 375 mL DMF. The solid product was sequentially rinsed with methanol and DMF before being dried in a vacuum oven at 120 °C for 24 h.

2.3. Sulfonation of PES polymer

To prepare sulfonated PES membranes, an electrophilic substitution reaction was carried out in this study. Chlorosulfonic acid was used as the sulfonating agent. 10 g of PES polymer was added into 100 mL dichloromethane in a three-necked round bottom flask. With continuous stirring and ice bath, 10 mL of chlorosulfonic acid (10% concentration) was added dropwise to the mixture above. The mixture was stirred for 2 h under nitrogen flow. After the reaction, the polymer was precipitated with 5-fold volume of ice-cold deionised water. The polymer was washed with deionised water until the pH reached 7. The obtained sulfonated PES was dried in vacuum oven at 60 °C for 24 h.

2.4. Preparation of mixed matrix membranes

All the mixed matrix PES and SPES membranes were prepared using phase inversion method. PES was dried in the oven at 105 °C before use. The compositions of the casting solutions for all the membranes are presented in Table 1. UiO-66 or UiO-66-NH_2 at different loadings (i.e., 5 wt% and 10 wt% based on the weight of polymer) was dispersed first in 16.8 mL DMAc and sonicated for 20 min. After that, 3.2 g SPES or PES polymer was added gradually into the dope solution to form a uniform and homogeneous solution by stirring for 24 h. The homogeneous solution was then left to stand in the fume hood for at least 24 h until no air bubbles were observed. The solution was then poured on a clean glass plate and cast using a doctor blade. The

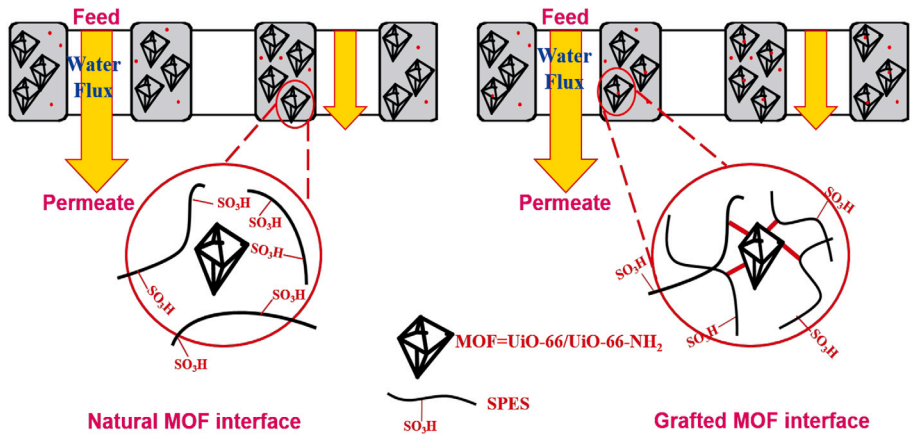

Fig. 1. Schematic diagram of MOFs and SPES mixed matrix membrane and the interaction between MOF and SPES.

Table 1
Compositions of the casting solution and resulting membrane. Binding indicates the MOF nanoparticles and polymers were chemically connected using chlorosulfonic acid as the coupling agent.

Membrane label	PES/SPES (g)	DMAc (mL)	UiO-66/ UiO-66-NH_2 (g)
Pristine PES	3.2 (16%)	16.80	0
SPES	3.2 (16%)	16.80	0
PES+UiO-66 (5%)	3.04 (16%)	16.80	0.16
PES+UiO-66 (10%)	2.88 (16%)	16.80	0.32
SPES+UiO-66 (5%)	3.04 (16%)	16.80	0.16
SPES+UiO-66(10%)	2.88 (16%)	16.80	0.32
SPES-UiO-66(5%) binding	3.04 (16%)	16.80	0.16
SPES-UiO-66(10%) binding	2.88 (16%)	16.80	0.32
PES+UiO-66-NH_2 (5%)	3.04 (16%)	16.80	0.16
PES+UiO-66-NH_2 (10%)	2.88 (16%)	16.80	0.32
SPES+UiO-66-NH_2 (5%)	3.04 (16%)	16.80	0.16
SPES+UiO-66-NH_2 (10%)	2.88 (16%)	16.80	0.32
SPES-UiO-66-NH_2 (5%) binding	3.04 (16%)	16.80	0.16
SPES-UiO-66-NH_2 (10%) binding	2.88 (16%)	16.80	0.32

glass plate was moved immediately to a deionised water bath at room temperature without any evaporation. After primary phase separation and membrane solidification, the prepared membranes were stored in fresh deionised water bath for 24 h. The resulting membranes were denoted as PES+UiO-66 (5%, 10%), SPES+UiO-66 (5%, 10%), SPES-UiO-66 (5%, 10%) binding, etc. Binding means the MOF nanoparticles and polymers were chemically crosslinked using chlorosulfonic acid as the coupling agent.

2.5. Characterisation of the synthesised MOFs

The morphologies of the prepared MOFs (UiO-66 and UiO-66-NH_2) were observed using scanning electron microscopy (SEM, Magellan SEM, FEI Company, America). The chemical compositions were characterised using Fourier transform infrared spectroscopy (FTIR, PerkinElmer 470). Powder X-ray diffraction (PXRD) patterns were conducted on a PANalytical X'Pert diffractometer using Cu kα radiation (λ=0.15406 nm). The current was 20 mA and the tube voltage was 35 kV. The XRD patterns were taken in the range of 5–80° at a scan speed of 2 °/min. Thermogravimetric analysis (TGA) was conducted under nitrogen atmosphere with a PerkinElmer thermal analysis instrument at a heating rate of 10 °C/min. The nitrogen adsorption–desorption, Brunauer–Emmett–Teller (BET) surface areas and pore volumes were carried out by Micromeritics, ASAP analyser at 77 K. The zeta potential measurements were carried out using Zetasizer Nano ZS90.

2.6. Characterisation of the prepared membranes

The surface composition of the mixed matrix membranes was characterised by FTIR at a resolution of 4 cm-1 and a range of 4000–600 cm^{-1}. The surface and cross-section morphologies of the mixed matrix membranes were characterised by SEM. The hydrophilicity of the membranes was measured using water contact angle (video-based optical contact angle measuring instrument, OCA-15EC, Dataphysics, Germany). To get more accurate results, at least five random locations were tested for each membrane sample and an average value was taken.

The porosity of the mixed matrix membranes was calculated using the gravimetric Eq. (1):

$$\epsilon(\%) = \frac{w_1 - w_2}{A \times l \times \rho_W} \times 100 \quad (1)$$

where w_1 and w_2 are the membrane weight after drying and before drying, A refers to membrane effective area, l refers to membrane thickness, ρ_w refers to water density.

Dead end cell filtration unit (HP4750 stirred cell, Sterlitech Corporation, USA) was used to determine the permeation water flux and retention ratio of all the prepared membranes. Membrane samples were cut and placed in the filtration cell. The cell was filled with 100 mL distilled water and then attached to small tank of 5 L of distilled water. Evaporating liquid nitrogen was employed to compact the system and control the feed pressure. During the filtration process, membrane samples are pre-compacted first at 150 kPa until the flux become stable. Then the pressure was reduced to 100 kPa and the flux was recorded using Labview software. The collected permeate was weighed using a digital balance and the flux was calculated using Eq. (2) [50] :

$$J_1 = \frac{M}{A\Delta t} \quad (2)$$

Where J_1 refers to permeation water flux, A refers to effective area, Δt refers to testing time, and M refers to weight of the collected permeate.

To determine the molecular weight cut-off (MWCO) and membrane pore size, a rejection test was conducted using polyethylene glycol (PEG) at different molecular weights. A 1 g/L of solution was prepared by dissolving PEG powder in water for 6 hr until the powder is completely dissolved. The PEG rejection rate is determined via a total organic analyser (TOC-LCSH, Shimadzu, Japan) using Eq. (3) [51]:

$$R(\%) = \left(1 - \frac{C_p}{C_f}\right) \times 100 \quad (3)$$

where R is the rejection rate, C_p and C_f are the concentrations of PEG solution in the permeate and feed, respectively.

The pore size of membranes can be calculated using Eq. (4) based on molecular weight cut-off values [52]:

$$r = 0.0262\sqrt{\text{MWCO}} - 0.3 \quad (4)$$

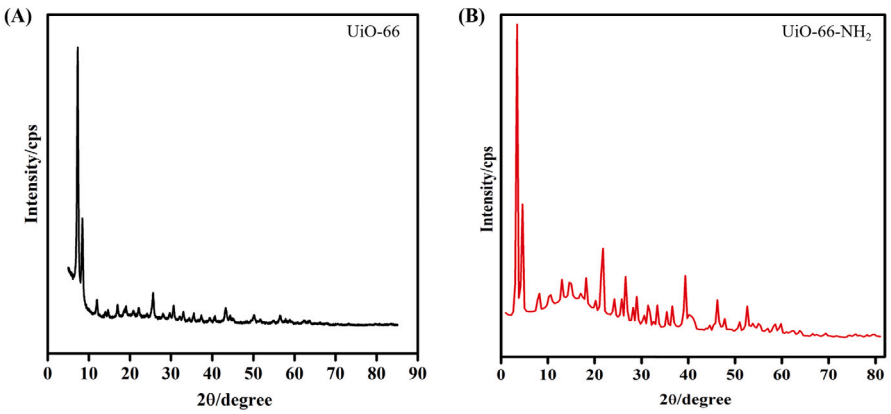

Fig. 2. PXRD of MOF UiO-66 and UiO-66-NH_2.

Where r is the pore size of membrane, MWCO is molecular weight cut-off that is estimated at 90% PEG rejection.

2.7. Anti-fouling properties of the prepared membranes

Anti-fouling properties of all prepared membranes were determined from constant transmembrane pressure (TMP) experiments using BSA as foulant. The membrane samples were pressurised using distilled water at 150 kPa for at least 60 min, then the distilled water was switched with the BSA solution (0.5 g/L) and the membrane was pressurised for 120 min. The flux of BSA was recorded at the last 10 min of the fouling process. The retention ratio of BSA (%R) was calculated similarly using Eq. (3)3). After that, the fouled membranes were removed from the filtration cell and washed with water. Physical and chemical cleaning were conducted to restore the flux. In physical cleaning, the fouled membranes were washed with distilled water for 20 min and the flux was recorded at 100 kPa. In chemical cleaning, the fouled membranes were washed with NaOH solution (2 g/L) for 20 min, followed by washing with distilled water three times to remove the NaOH solution and the flux was recorded at 100 kPa. For each cleaning cycle, the flux was recorded at 100 kPa. Three cycles of fouling were conducted for each membrane sample to get accurate and reliable data. To determine membrane performance, flux recovery ratio was calculated using Eq. (5) [50]:

$$\mathrm{FRR}(\%) = \frac{J_{w2}}{J_{w1}} \times 100 \tag{5}$$

Where FRR refers to flux recovery ratio, J_{w2} and J_{w1} are the flux after the cleaning process and before the fouling process, respectively.

To investigate the details of membrane fouling, total fouling resistance (R_t), reversible fouling resistance (R_r) and irreversible fouling resistance (R_{ir}) were calculated using Eqs. (6)–(8) [48], respectively:

$$R_t = \frac{J_{w1} - J_p}{J_{w1}} \times 100 \tag{6}$$

$$R_r = \frac{J_{w2} - J_p}{J_{w1}} \times 100 \tag{7}$$

$$R_{ir} = \frac{J_{w1} - J_{w2}}{J_{w1}} \times 100 \tag{8}$$

Where J_p is the flux of BSA model foulant, J_{w2} and J_{w1} are the flux after cleaning process and before fouling process, respectively, R_t is the sum of R_r and R_{ir}.

2.8. Membrane stability test

Long-term usage of membranes is very important for commercial applications. The performance of membranes deteriorates during their lifespan. Therefore, the stability test was undertaken to check the performance of membranes after a long period of time. The stability test was done using physical stability. In this part, the PES, SPES and mixed matrix membranes were immersed in distilled water at room temperature for a period of 3 months, 6 months and 12 months. The water was changed daily. Then the stability was measured in terms of membrane performance, membrane morphology, membrane hydrophilicity and anti-fouling performance.

3. Results and discussion

Characterisation of the synthesised MOFs

The PXRD spectra for UiO-66 (Fig. 2A). showed 8 major peaks at 7.3°, 8.44°, 11.9°, 21°, 25.6°, 30.7°, 31°, 43.3°, 50.1° and 56.4°, indicating that UiO-66 was a highly crystalline structure. UiO-66-NH_2 (Fig. 2B). showed 8 major peaks at 3.4°, 4.6°, 18.2°, 21.8°, 26.6°, 39.4°, 46.2° and 52.6°. The PXRD results of UiO-66-NH_2 and UiO-66 matched well with the reported results in the literature and confirmed the successful synthesis of the MOFs [53–55].

The SEM morphology of UiO-66 and UiO-66-NH_2 is shown in Fig. 3. The crystals of UiO-66-NH_2 formed a roughened spherical shape and the average particle diameter was approximately 50 nm. By contrast, the crystals of UiO-66 had a ball shape and the particle diameter was around 30 nm.

FTIR spectra for UiO-66-NH_2 and UiO-66 are shown in Fig. 4A. The absorption peaks at 1665 cm^{-1} ,1556 cm^{-1} and 1503 cm^{-1} corresponded to the C=O symmetric stretching in the carboxylate group of the terephthalic acid, the O-C-O asymmetric stretching in the terephthalic acid and the typical vibration present in the C=C stretching of benzene ring, respectively [56]. The peak value of UiO-66 between the ranges of 3000–3600 cm^{-1} showed the presence of the -OH group. Compared with the FTIR spectrum of UiO-66, the 3457 cm^{-1} and 3357 cm^{-1} peaks in the spectrum of UiO-66-NH_2 were due to the asymmetrical, symmetrical and stretching vibrations of the -NH_2 group [57, 58]. The peaks at 1336 cm^{-1} and 1420 cm^{-1} were ascribed to the C-N stretching vibration of aromatic amines and the N-H bending vibration, respectively [58]. The FTIR spectrum of UiO-66-NH_2 confirmed the successful functionalisation of amine groups.

The BET surface areas of UiO-66 and UiO-66-NH_2 were measured using nitrogen adsorption–desorption isotherms and the results are shown in Table S1. The BET surface area of the synthesised UiO-66-NH_2 was lower (927.5 m^2/g) than that of native UiO-66 (1216 m^2/g) due to the presence of -NH_2 functional groups in the porous structure. Likewise, the micropore volume of UiO-66-NH_2 (0.466 cm^3/g) was lower than that of UiO-66 (1.54 cm^3/g). These data are consistent with those reported in the literature [59,60].

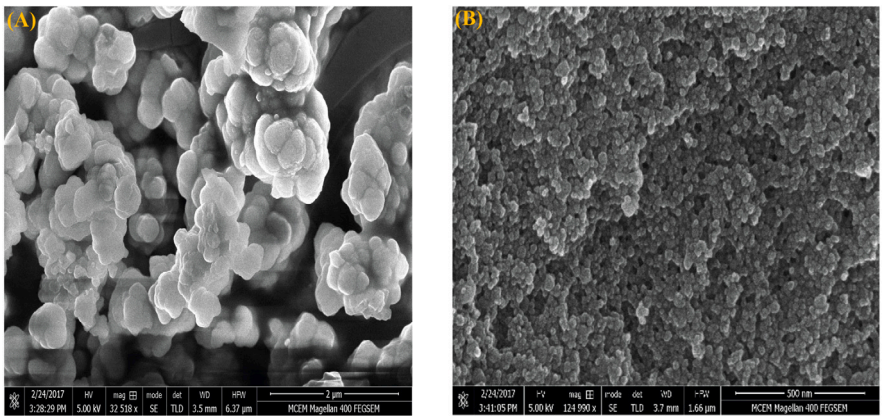

Fig. 3. SEM images of MOF UiO-66 and UiO-66-NH_2.

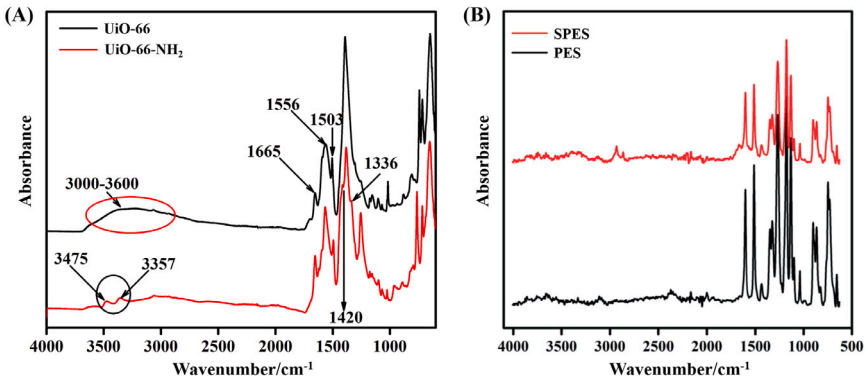

Fig. 4. FTIR spectra of UiO-66 and UiO-66-NH_2.

3.1. Membrane characterisation

Fig. 4B showed the FTIR spectrum for PES and SPES membranes. Symmetrical and asymmetrical stretching vibrations of sulfonic acid groups normally appear at 1028 and 1180 cm^{-1}. The peak at 1028 cm^{-1} was observed which was assigned to the symmetrical stretching vibrations of sulfonic acid groups or sulfonate groups whilst, the peak at 1180 cm^{-1} which is assigned to the asymmetrical stretching vibrations of sulfonic acid groups was not be observed due to the presence of other overlapping absorbances.

The presence of the MOF nanoparticles in the membranes was confirmed by PXRD at 2θ ranging of 10° to 80° (Figure S2 A and B for both MOFs). Pristine PES membrane is primarily amorphous and show only one diffraction peak at 2θ =18.32°, which is the same for the all mixed matrix PES membranes. SPES membranes also show only one diffraction peak at 2θ =18.32°, which is the same as pristine PES membranes. The difference between PES and SPES is only in peak intensity. After incorporation of UiO-66-NH_2 to the PES casting solution, the diffraction peaks at 2θ = 1°, 4.6°, 18.2° and 21.8° were observed. These peaks were roughly similar to the peaks in UiO-66-NH_2. These results confirmed the presence of UiO-66-NH_2 within the membrane surfaces. The same observation was obtained for UiO-66. The diffraction peaks at 2θ = 7.5° are similar to those of UiO-66. This result confirmed the presence of UiO-66 within the membrane surface.

3.2. Membrane surface hydrophilicity

Membrane surface hydrophilicity is regarded as an important factor in determining the membrane flux and membrane performance [61]. Higher membrane surface hydrophilicity means higher permeation flux and higher anti-fouling performance [62]. The hydrophilicity of membranes is measured by water contact angle. As shown in Fig. 5, pristine PES membranes showed the highest contact water angle (80°) due to the inherent hydrophobic property of PES. After sulfonation of PES membranes with chlorosulfonic acid, the water contact angle was reduced to 59.2° which was about 26% lower than the pristine membrane. The reduction in water contact angle was due to the strong hydrogen bonding between the water molecules and membrane surface due to the presence of polar groups of SO_3H which were strongly hydrophilic. This result agreed well with the previous reported results [63]. Furthermore, when MOFs were incorporated in the membranes, the contact angle decreased. More research is needed to uncover the mechanism of hydrophobic MOFs in decreasing contact angles and increasing membrane hydrophilicity. One possible reason could be that UiO-66 possessed hydrophilic pore which was appropriate for water filtration [56,64,65], and UiO-66-NH_2 has hydrophilic character due to presence of the -NH_2 functional groups [66–68].

The addition of MOF nanoparticles in the casting solutions improved the surface hydrophilicity of the mixed matrix membranes. The reduction in membrane contact angle confirmed the improvement in membrane hydrophilicity, which came from the innate high hydrophilicity of the nanoparticles [41]. Addition of 5% and 10% loading of UiO-66-NH_2 NPs to the PES casting solutions decreased the contact angle from 80° for pristine PES to 44° and 34.7° for the resulting mixed matrix membranes, respectively. This reduction may be ascribed to surface enrichment with amino -NH_2 groups. The amine groups in the MOF can offer strong attraction force (hydrogen bonding) with water molecules, which enhanced the hydrophilicity of the modified membranes. On the other hand, it was postulated that introduction of hydrophilic nanoparticles into PES casting solutions accelerated the exchange rate between solvent (i.e., DMAc) and non-solvent (i.e., distilled water) during the phase inversion method, resulting in porous structure of the mixed matrix membranes [32,41,69,70]. After addition

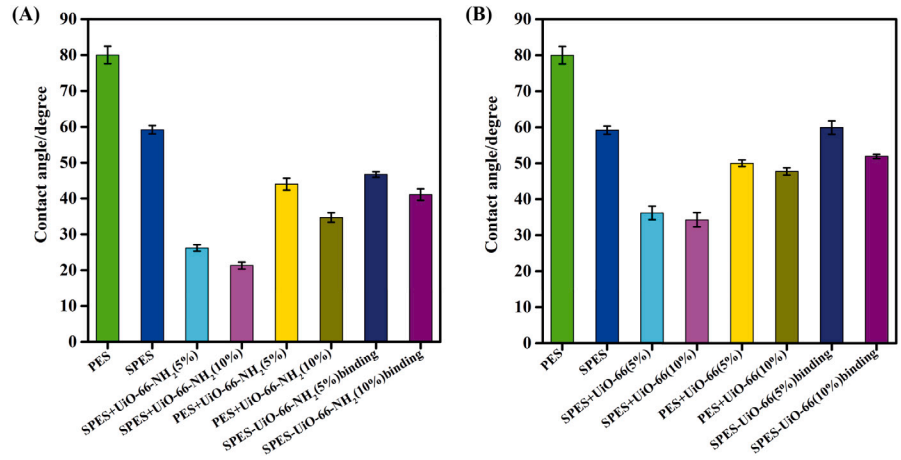

Fig. 5. Contact angle of pristine membranes and mixed matrix membranes after incorporation of UiO-66 and UiO-66-NH_2. The bar height is the average of five contact angle measurements for each membrane sample. The error bars represent one standard deviation.

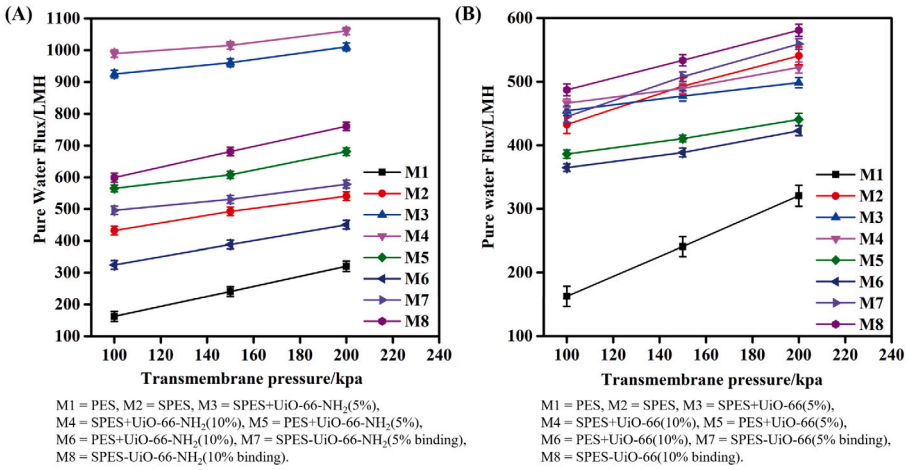

Fig. 6. Pure water flux of pristine membranes and mixed matrix membranes after incorporation of UiO-66 and UiO-66-NH_2 under different transmembrane pressures.

of UiO-66-NH_2 nanoparticles to the SPES membranes at loadings of 5% and 10%, the water contact angle also reduced from 59.2° for SPES membranes to 26.2° and 21.3° for SPES+UiO-66-NH_2 membranes and 49.9° and 41.9° for SPES-UiO-66-NH_2 binding membranes, respectively. Similarly, this reduction was due to the presence of hydrophilic porous nanoparticles.

As shown in Fig. 5, after incorporating UiO-66 into PES and SPES casting solution, the hydrophilicity of the mixed matrix membranes was also improved due to introduction of hydrophilic -COOH functional groups through the attachment/embedding of UiO-66 to the casting solutions. In the phase inversion process, the UiO-66 moved potentially to the interface between the casting solution and the water bath. As a result, the hydrophilic carboxyl functional groups occurred on the surface of membranes which improved the surface hydrophilicity [69–71].

3.3. Anti-fouling performance of membranes

Pure water flux and rejections are two important factors evaluating the antifouling performance of membranes. The water fluxes of membranes were tested at different filtration pressures ranging from 100 kPa, 150 kPa and 200 kPa. The results were presented in Fig. 6. Pristine PES membranes showed the lowest water flux among all the membranes. Generally, pure water flux of the membranes increased with increasing transmembrane operating pressure, which was reasonable due to the increasing driving force. Besides, when all the other conditions were kept the same, the sulfonated membranes generally showed higher water flux compared to unsulfonated membranes, such as M2 versus M1, M3 versus M5, and M4 versus M6, which was possibly due to the hydrophilic property of the sulfonate groups. In addition, membranes incorporating UiO-66-NH_2 generally demonstrated higher pure water flux compared to membranes incorporating UiO-66, which was possibly attributed to the more hydrophilic property of UiO-66-NH_2 compared to UiO-66. As a result, it was reasonable that SPES+UiO-66-NH_2 (5% and 10%) membranes showed highest water flux among all the membranes. However, it should be pointed out that the small pore size of the modified membranes was not commensurate with their high permeation flux, which indicated that permeation flux was influenced by other factors as well, and more efforts are needed to uncover the underlying mechanism in the future.

The results of pure water flux of the pristine and mixed matrix membranes after incorporating of two fillers (UiO-66-NH_2 and UiO-66) are illustrated in Fig. 7. Pristine PES membrane possessed lower pure water flux (162.4 L/m^2/h or LMH) due to the hydrophobic nature of polymers matrix. After sulfonating PES with chlorosulfonic acid, the water flux of SPES membrane increased rapidly (432.6 LMH, about 70% increment) due to the increase of membranes hydrophilicity as confirmed by the results of contact angle and due to the presence of -SO_3H groups that was strongly hydrophilic. After adding different concentrations of UiO-66-NH_2 to the SPES casting solution, the water flux has increased remarkably, and reaches a maximum of 665.5 and 678.0 LMH at SPES+UiO-66-NH_2 content of 5% and 10%, which is

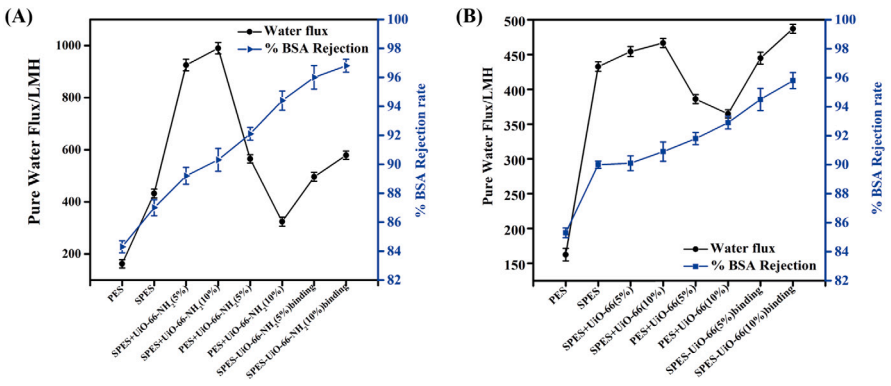

Fig. 7. Pure water flux and BSA rejection of pristine membranes and mixed matrix membranes after incorporation of UiO-66 and UiO-66-NH2 at pressure of 100 kPa.

four times that of pristine PES and 1.5 times of SPES membranes. This due to strong hydrogen bonds between water molecules and the membrane surface due to presence of hydrophilic UiO-66-NH_2 nanoparticles. In addition, the water permeation flux of PES+UiO-66-NH_2 (5%) membranes was increased after introducing UiO-66-NH_2 to the casting solution (about 565 LMH). However, it decreased upon addition of a larger amount of UiO-66-NH2 (10%, about 324.3 LMH). The reason could be related to pore blocking with higher loadings of the nanoparticles, which agrees well with the decrease in membrane porosity and membrane pore size [23,72,73].

Furthermore, regarding UiO-66, SPES-UiO-66 (10% binding) membranes exhibited higher water permeation flux (about 487.1 LMH) compared to other membranes, which was 66% higher than pristine PES and 11% higher than SPES membranes. The reason for the improvement in water permeation flux could be ascribed to the presence of polar groups of SPES and functional carboxylic acid groups (-COOH) of UiO-66. Similarly, the water permeation flux of SPES+UiO-66 (5% and 10%) membranes was higher than SPES membranes due to increased membrane surface hydrophilicity and presence of -COOH functional groups.

Generally, the improvement of membrane flux after incorporation of UiO-66-NH_2 to PES/SPES membranes was higher than after incorporation of UiO-66 to PES/SPES membranes because the interaction or dispersion of UiO-66-NH2 nanoparticles within PES/SPES polymers was better. Incorporating UiO-66-NH2 into the casting solution would cause a rapid phase inversion process, consequently leading to an accelerated exchange rate between solvent and non-solvent. Furthermore, the presence of UiO-66-NH_2 nanoparticles in the casting solution would diminish the interaction of polymer chains and increase the dispersion due to their inorganic constituent, thereby reducing the compactness and density of the skin layer. In summary, the above results illustrated that UiO-66 and UiO-66-NH_2 are favourable fillers for the fabrication of UF membranes with high membrane flux.

The rejection of BSA (model foulant) is shown in Fig. 7. The rejections of all the mixed matrix membranes after incorporating two fillers (UiO-66 and UiO-66-NH_2) showed a gradual increase compared to PES membrane, which was due to the change in pore size, porosity, as well as the charges of the solute and the membrane surface. Small pore size and decreased porosity could increase BSA rejection. In addition, it was possible that both the BSA and the mixed matrix membrane surface possessed a negative charge, and therefore the repulsion between BSA and membrane increased, resulting a higher BSA rejection. Furthermore, the surfaces of mixed matrix membranes were more hydrophilic because of the presence of amine functional groups (-NH_2) for UiO-66-NH_2 and carboxylic functional groups (-COOH) for UiO-66 on the surface of mixed matrix membranes. This was confirmed by the results of contact angles as discussed earlier. As a result of the interactions between the functional groups and water molecules, the water molecules were attached readily to the membrane surfaces and formed a thin hydration layer between the membrane surfaces and foulants (e.g. BSA). This layer would not only increase the membrane flux but also would deter the adsorption of BSA protein on the surface of membrane.

Figure S3 shows the fouling behaviour of the prepared membranes. It can be observed that the permeation flux of the BSA solution decreased significantly in comparison with the initial water flux at the initial stages because of the protein fouling. During the filtration process of the BSA solution, the BSA protein tends to deposit on the surface of membranes and be entrapped in the membrane pores, leading to pore blocking. Thus, the water flux of the mixed matrix membranes after physical and chemical cleaning could be recovered totally to its initial values. The reason maybe because of embedding a hydrophilic nanoparticle into the membrane matrix which leads to enhance membrane hydrophilicity as confirmed by the results of water contact angle.

Flux recovery ratio (FRR) is another important aspect in determining the reusability and performance of the membranes. A greater FRR indicates a better anti-fouling property. The FRR for pristine and mixed matrix membranes were shown in Fig. 8. It can be seen that pristine PES membrane showed lower FRR (44.5%) due to the hydrophobic character. The FRR for mixed matrix PES membranes was increased gradually after addition of MOF nanoparticles. The best membrane performance in terms of FRR was observed for SPES-UiO-66-NH_2 (10% binding) and SPES-UiO-66 (10% binding), respectively. Generally, all mixed matrix membranes showed high anti-fouling property, due to the increase of membrane hydrophilicity.

To observe quantitatively the membrane fouling performance, total filtration resistance (R_t), intrinsic membrane resistance (R_m), reversible resistance (R_r) due to the external deposition of pollutants on the membrane surface, and irreversible resistance (R_{ir}) due to the strong adherence of pollutants on the membrane surface were studied and the results are presented in Table S3. The mixed matrix membranes for both MOFs suffered more reversible fouling than irreversible fouling due to the fact that higher transmembrane pressure (TMP) was required during the fouling experiments due to lower pore size of the membranes. The variations in R_r and R_{ir} were pronounced. The R_r was increased while the R_{ir} was decreased. Compared to the pristine PES membranes, the ratio of R_r/R_t was increased while the ratio of R_{ir}/R_t was decreased for mixed matrix membranes, indicating that the foulant adsorbed on the top surface of the membranes could be more easily washed off during the cleaning process. Therefore, a better anti-fouling performance was achieved.

Static protein absorption (BSA adsorption) is one of the main features in determining the anti-fouling performance of membranes and the reduction of foulant on the membrane surface indicates better anti-fouling performance of the membranes [74]. The results of static protein adsorption for PES, SPES and mixed matrix membranes were presented in Fig. 9. Pristine PES membranes showed highest static protein adsorption. In other words, mixed matrix PES and SPES membranes exhibited higher resistance to BSA protein than the pristine PES

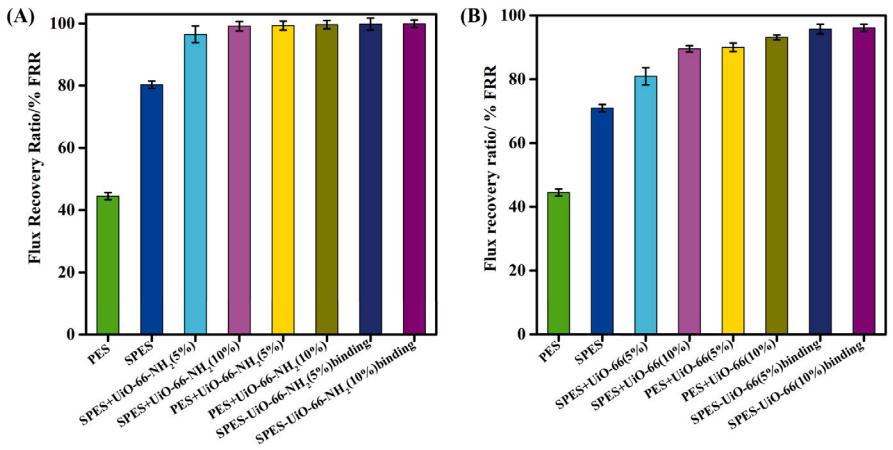

Fig. 8. Flux recovery ratio of pristine membranes and mixed matrix membranes after incorporation of UiO-66 and UiO-66-NH_2.

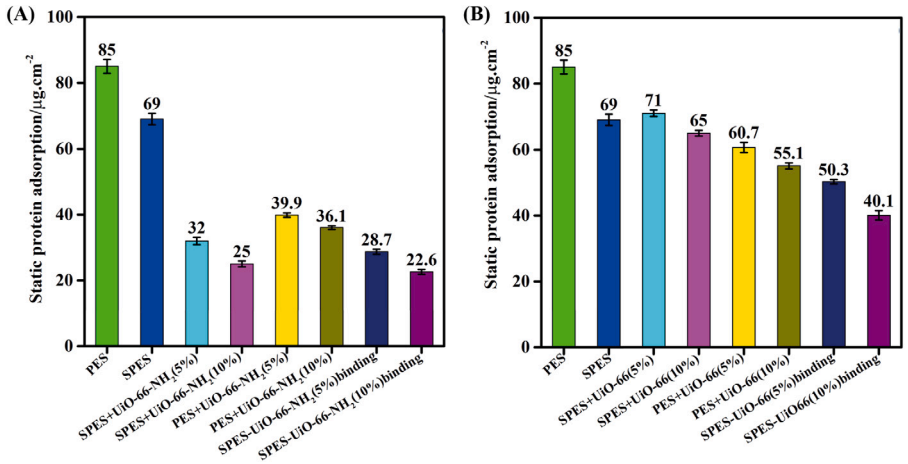

Fig. 9. Static protein absorption of pristine membranes and mixed matrix membranes after incorporation of UiO-66 and UiO-66-NH_2.

membranes due to the change in pore size, porosity, charge of the solute and membrane surface, as well as the presence of hydrophilic moieties of UiO-66 and UiO-66-NH_2 within the membrane matrix. Additionally, the hydrophilic functional groups of the two MOFs (UiO-66 and UiO-66-NH_2) in the mixed matrix membranes might regularly form a buffer layer on the membrane surface via hydrogen bond, and the BSA foulant was eliminated from the formed buffer layer to avoid the substantial entropy loss caused by the entrance of large molecules of protein into the surface of membrane [74]. Generally, there was not a clear trend among the different series of mixed matrix membranes in terms of static protein adsorption, but it seemed that when all the other conditions were kept the same, increasing the loading of MOFs had a negative effect on static protein adsorption.

3.4. Long-term stability

The PES, SPES and mixed matrix membranes were immersed in distilled water at room temperature for a period of 3 months, 6 months and 12 months. To examine the physical stability of membrane performance, the contact angle was measured and the results are shown in Fig. 10. It can be seen that the contact angle of mixed matrix membranes for both MOFs did not change significantly in comparison with the fresh mixed matrix membranes, indicating that the mixed matrix membranes maintained the hydrophilic property after long-term storage in water.

The pure water flux of virgin PES and mixed matrix membranes was also measured and the results were shown in Fig. 11. The changes in water flux were more than 10% in some samples of membranes. For example, SPES+UiO-66-NH_2 (10%) membranes showed a difference of more than 100 LMH after 12 months storage. Likewise, almost all the UiO-66 samples showed flux changes of 10% after 12 months. Regarding the percentage rejection of BSA, the results are presented in Table S4 and Table S5 for virgin PES and mixed matrix membranes. The changes in percentage rejection of BSA for both MOFs were around 3% after 12 months. The FRR for mixed matrix membranes was also measured and the results are summaries in Tables S6 and S7. The difference between membranes after 12 months and fresh membranes was insignificant. Furthermore, as revealed by the results of static protein adsorption shown in Tables S8 and S9, no distinct difference was observed for mixed matrix membranes after storing in water.

In order to further confirm the presence of MOFs within the membranes after 12 months, the EDX of the mixed matrix membranes was taken and the results are shown in Fig. 12. It was observed that the Zr peak was very distinct, which came from the MOFs. These results indicated that MOFs still remained within the membrane matrix after long term storage in water. The long-term operational stability of mixed matrix UF membranes was evaluated to investigate the life of the reusable membranes to confirm that the membrane will not collapse or destroy over long-period during the filtration process, where it can affect the products and even the process itself. BSA was used as model foulant (1 mg/l) at 25 °C and a transmembrane pressure of 3 bar. SPES+UiO-66-NH_2 (5% and 10%), SPES+UiO-66(5%), and SPES-UiO-66 (5% binding) membranes were selected as they represented the optimum membranes among the all mixed matrix membranes, and the results are shown in

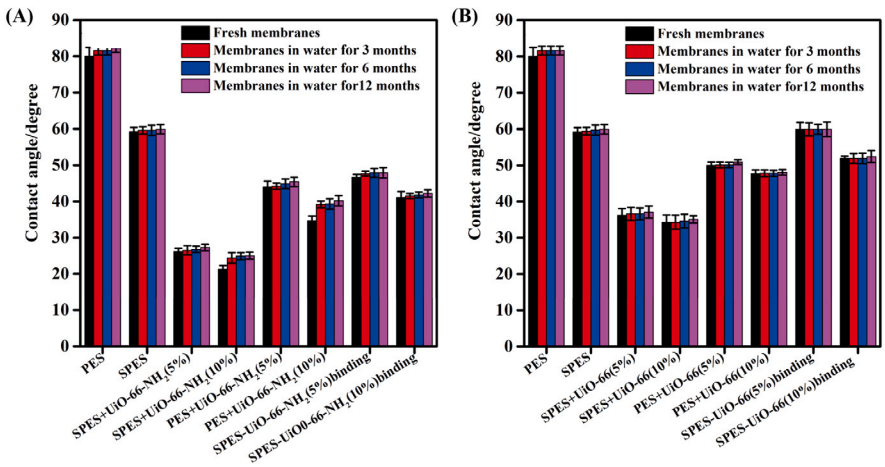

Fig. 10. Contact angle of pristine membranes and mixed matrix membranes after immersing membranes in water for 3 months, 6 months and 12 months.

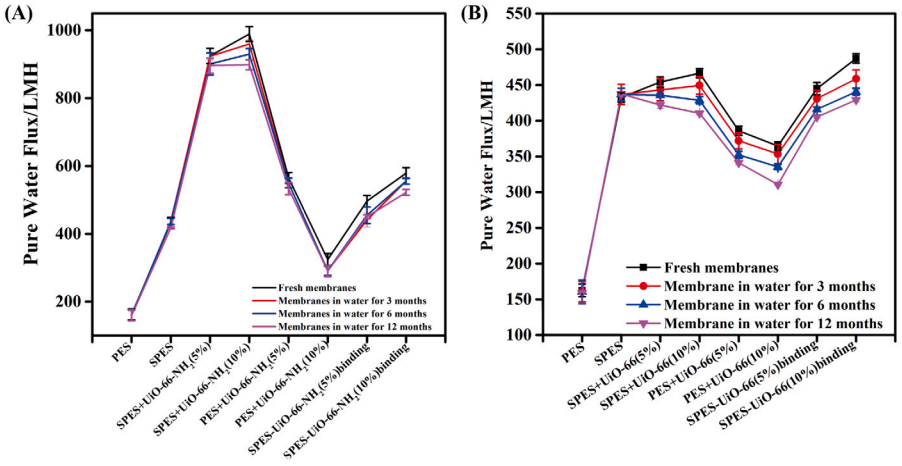

Fig. 11. Pure water flux of pristine membranes and mixed matrix membranes after immersing membranes in water for 3 months, 6 months and 12 months.

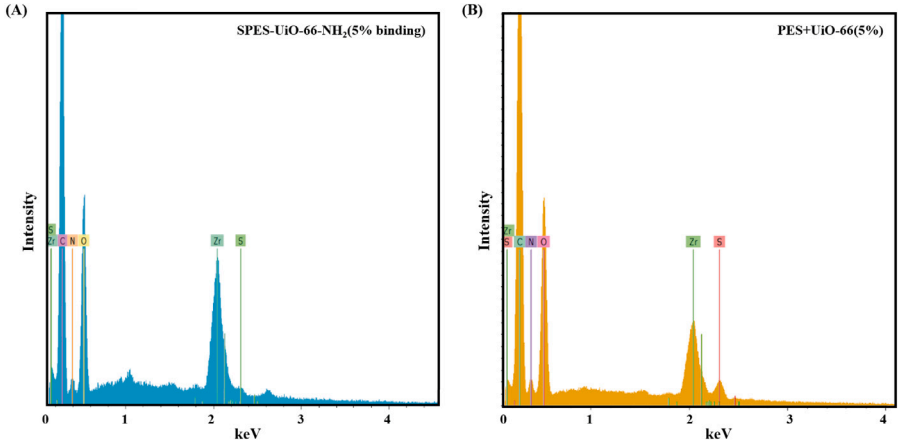

Fig. 12. EDX of mixed matrix membranes after immersing membranes in water for 12 months.

Figure S4. It can be seen that a sharp decline was observed for PES UF membranes from 14 LMH to 6 LMH during 26 days of filtration process, which is due to the hydrophobic character. However, the mixed matrix membranes showed great stability after long-term operation for both MOFs. The permeation flux of the SPES+UiO-66-NH2 (5% and 10%) using BSA solution was stable throughout the UF operation between 31.7 and 31.0 LMH and 43.8 and 42.0 LMH respectively. For UiO-66, the permeation flux of SPES+UiO-66 (5%) and SPES-UiO-66 (5% binding) membranes were stable during the 26 days between 23.7 and 23.5 LMH for SPES+UiO-66 (5%) and 25.5 and 26.06 LMH for SPES-UiO-66 (5% binding). The main reason for stable and long performance during the long-term UF operation was the embedding of hydrophilic nanoparticle (UiO-66-NH_2 and UiO-66) in the membrane matrix.

4. Conclusions

In this work, UiO-66-NH_2 and UiO-66 MOFs were synthesised and incorporated in the PES and SPES casting solutions to fabricate mixed matrix membranes via phase inversion method. The embedding of both MOFs improved the membrane hydrophilicity. Moreover, the presence of hydrophilic MOFs in the membranes provided additional flow channels for water permeation. Overall, the mixed matrix membranes showed higher membrane flux, higher BSA rejection and higher antifouling properties compared to pristine PES and SPES membranes. Also, the MOFs could stably stay in the mixed matrix membranes for a long time due to the high stability of MOFs in water. The mixed matrix membranes also showed great stability during long-term operation test. Therefore, the outstanding performance of the resulting mixed matrix membranes highlighted the promising potential of UiO-66-NH_2 and UiO-66 in the development of stable and permanent hydrophilic ultrafiltration membranes for applications of water and wastewater treatment.

CRediT authorship contribution statement

Muayad Al-Shaeli: Conceptualization, Investigation, Writing. **Stefan J.D. Smith:** Methodology, Supervision. **Shanxue Jiang:** Methodology, Writing. **Huanting Wang:** Conceptualization, Supervision. **Kaisong Zhang:** Conceptualization, Supervision. **Bradley P. Ladewig:** Conceptualization, Supervision, Writing, Resources.

Declaration of competing interest

The authors declare that they have no known competing financial interests or personal relationships that could have appeared to influence the work reported in this paper.

Acknowledgement

Muayad Al-Shaeli acknowledges funding support from the Iraqi Government.

Appendix A. Supplementary data

Supplementary material related to this article can be found online at https://doi.org/10.1016/j.memsci.2021.119339.

References

[1] S. Yang, Q. Zou, T. Wang, L. Zhang, Effects of GO and MOF@GO on the permeation and antifouling properties of cellulose acetate ultrafiltration membrane, J. Membr. Sci. 569 (2019) 48–59, https://doi.org/10.1016/j.memsci.2018.09.068.

[2] K.P. Lee, T.C. Arnot, D. Mattia, A review of reverse osmosis membrane materials for desalination-development to date and future potential, J. Membr. Sci. 370 (1–2) (2011) 1–22, https://doi.org/10.1016/j.memsci.2010.12.036.

[3] S. Jiang, Y. Li, B.P. Ladewig, A review of reverse osmosis membrane fouling and control strategies, Sci. Total Environ. 595 (2017) 567–583, https://doi.org/10.1016/j.scitotenv.2017.03.235, http://linkinghub.elsevier.com/retrieve/pii/S0048969717307660.

[4] S. Hube, M. Eskafi, K.F. Hrafnkelsdóttir, B. Bjarnadóttir, M.Á. Bjarnadóttir, S. Axelsdóttir, B. Wu, Direct membrane filtration for wastewater treatment and resource recovery: A review, Sci. Total Environ. 710 (2020) 136375, https://doi.org/10.1016/j.scitotenv.2019.136375.

[5] T. Ahmad, C. Guria, A. Mandal, A review of oily wastewater treatment using ultrafiltration membrane: A parametric study to enhance the membrane performance, J. Water Process Eng. 36 (June) (2020) 101289, https://doi.org/10.1016/j.jwpe.2020.101289.

[6] S. Jiang, B. Ladewig, Green synthesis of polymeric membranes: Recent advances and future prospects, Curr. Opin. Green Sustain. Chem. 21 (2020) 1–8, https://doi.org/10.1016/j.cogsc.2019.07.002.

[7] Z. Wang, R. Sahadevan, C. Crandall, T.J. Menkhaus, H. Fong, Hot-pressed PAN/PVDF hybrid electrospun nanofiber membranes for ultrafiltration, J. Membr. Sci. 611 (May) (2020) 118327, https://doi.org/10.1016/j.memsci.2020.118327.

[8] F. Qu, H. Liang, J. Zhou, J. Nan, S. Shao, J. Zhang, G. Li, Ultrafiltration membrane fouling caused by extracellular organic matter (EOM) from microcystis aeruginosa: Effects of membrane pore size and surface hydrophobicity, J. Membr. Sci. 449 (2014) 58–66, https://doi.org/10.1016/j.memsci.2013.07.070.

[9] L. Shao, Z.X. Wang, Y.L. Zhang, Z.X. Jiang, Y.Y. Liu, A facile strategy to enhance PVDF ultrafiltration membrane performance via self-polymerized polydopamine followed by hydrolysis of ammonium fluotitanate, J. Membr. Sci. 461 (2014) 10–21, https://doi.org/10.1016/j.memsci.2014.03.006.

[10] X. Lin, K. Wang, Y. Feng, J.Z. Liu, X. Fang, T. Xu, H. Wang, Composite ultrafiltration membranes from polymer and its quaternary phosphonium-functionalized derivative with enhanced water flux, J. Membr. Sci. 482 (2015) 67–75, https://doi.org/10.1016/j.memsci.2015.02.017.

[11] X. Shi, G. Tal, N.P. Hankins, V. Gitis, Fouling and cleaning of ultrafiltration membranes: A review, J. Water Process Eng. 1 (2014) 121–138, https://doi.org/10.1016/j.jwpe.2014.04.003.

[12] Q. Li, J. Imbrogno, G. Belfort, X.L. Wang, Making polymeric membranes antifouling via "grafting from" polymerization of zwitterions, J. Appl. Polym. Sci. 132 (21) (2015) https://doi.org/10.1002/app.41781.

[13] H. Susanto, M. Ulbricht, High-performance thin-layer hydrogel composite membranes for ultrafiltration of natural organic matter, Water Res. 42 (10–11) (2008) 2827–2835, https://doi.org/10.1016/j.watres.2008.02.017.

[14] Q. Shi, Y. Su, S. Zhu, C. Li, Y. Zhao, Z. Jiang, A facile method for synthesis of pegylated polyethersulfone and its application in fabrication of antifouling ultrafiltration membrane, J. Membr. Sci. 303 (1–2) (2007) 204–212, https://doi.org/10.1016/j.memsci.2007.07.009.

[15] M. Rahimi, S. Zinadini, A.A. Zinatizadeh, V. Vatanpour, L. Rajabi, Z. Rahimi, Hydrophilic goethite nanoparticle as a novel antifouling agent in fabrication of nanocomposite polyethersulfone membrane, J. Appl. Polym. Sci. 133 (26) (2016) https://doi.org/10.1002/app.43592.

[16] L. Yang, B. Tang, P. Wu, UF Membrane with highly improved flux by hydrophilic network between graphene oxide and brominated poly(2,6-dimethyl-1,4-phenylene oxide), J. Mater. Chem. A 2 (43) (2014) 18562–18573, https://doi.org/10.1039/c4ta03790a.

[17] S.J. Lee, M. Dilaver, P.K. Park, J.H. Kim, Comparative analysis of fouling characteristics of ceramic and polymeric microfiltration membranes using filtration models, J. Membr. Sci. 432 (2013) 97–105, https://doi.org/10.1016/j.memsci.2013.01.013.

[18] C. Ba, D.A. Ladner, J. Economy, Using polyelectrolyte coatings to improve fouling resistance of a positively charged nanofiltration membrane, J. Membr. Sci. 347 (1–2) (2010) 250–259, https://doi.org/10.1016/j.memsci.2009.10.031.

[19] R.F. Susanti, Y.S. Han, J. Kim, Y.H. Lee, R.G. Carbonell, A new strategy for ultralow biofouling membranes: Uniform and ultrathin hydrophilic coatings using liquid carbon dioxide, J. Membr. Sci. 440 (2013) 88–97, https://doi.org/10.1016/j.memsci.2013.03.068.

[20] M. Peyravi, A. Rahimpour, M. Jahanshahi, A. Javadi, A. Shockravi, Tailoring the surface properties of PES ultrafiltration membranes to reduce the fouling resistance using synthesized hydrophilic copolymer, Micropor. Mesopor. Mater. 160 (2012) 114–125, https://doi.org/10.1016/j.micromeso.2012.04.036.

[21] A. Rahimpour, UV Photo-grafting of hydrophilic monomers onto the surface of nano-porous PES membranes for improving surface properties, Desalination 265 (1–3) (2011) 93–101, https://doi.org/10.1016/j.desal.2010.07.037.

[22] M.N. Seman, M. Khayet, N. Hilal, Comparison of two different UV-grafted nanofiltration membranes prepared for reduction of humic acid fouling using acrylic acid and N-vinylpyrrolidone, Desalination 287 (2012) 19–29, https://doi.org/10.1016/j.desal.2010.10.031.

[23] V. Vatanpour, S.S. Madaeni, A.R. Khataee, E. Salehi, S. Zinadini, H.A. Monfared, TiO2 embedded mixed matrix PES nanocomposite membranes: Influence of different sizes and types of nanoparticles on antifouling and performance, Desalination 292 (2012) 19–29, https://doi.org/10.1016/j.desal.2012.02.006.

[24] V. Vatanpour, S.S. Madaeni, L. Rajabi, S. Zinadini, A.A. Derakhshan, Boehmite nanoparticles as a new nanofiller for preparation of antifouling mixed matrix membranes, J. Membr. Sci. 401–402 (2012) 132–143, https://doi.org/10.1016/j.memsci.2012.01.040.

[25] Q. Shi, Y. Su, W. Chen, J. Peng, L. Nie, L. Zhang, Z. Jiang, Grafting short-chain amino acids onto membrane surfaces to resist protein fouling, J. Membr. Sci. 366 (1–2) (2011) 398–404, https://doi.org/10.1016/j.memsci.2010.10.032.

[26] F. Shi, Y. Ma, J. Ma, P. Wang, W. Sun, Preparation and characterization of PVDF/TiO2 hybrid membranes with ionic liquid modified nano-TiO2 particles, J. Membr. Sci. 427 (2013) 259–269, https://doi.org/10.1016/j.memsci.2012.10.007.

[27] X. Zhang, Y. Wang, Y. Liu, J. Xu, Y. Han, X. Xu, Preparation, performances of PVDF/ZnO hybrid membranes and their applications in the removal of copper ions, Appl. Surf. Sci. 316 (1) (2014) 333–340, https://doi.org/10.1016/j.apsusc.2014.08.004.

[28] Z. Sun, H. Chen, X. Ren, Z. Zhang, L. Guo, F. Zhang, H. Cheng, Preparation and application of zinc oxide/poly(m-phenylene isophthalamide) hybrid ultrafiltration membranes, J. Appl. Polym. Sci. 136 (22) (2019) https://doi.org/10.1002/app.47583.

[29] Z. Rahimi, A.A.L. Zinatizadeh, S. Zinadini, Preparation of high antibiofouling amino functionalized MWCNTs/pes nanocomposite ultrafiltration membrane for application in membrane bioreactor, J. Ind. Eng. Chem. 29 (2015) 366–374, https://doi.org/10.1016/j.jiec.2015.04.017.

[30] M.S. Muhamad, M.R. Salim, W.J. Lau, Preparation and characterization of PES/SiO2 composite ultrafiltration membrane for advanced water treatment, Korean J. Chem. Eng. 32 (11) (2015) 2319–2329, https://doi.org/10.1007/s11814-015-0065-3.

[31] E. Tomczak, M. Blus, Preparation and permeability of PVDF membranes functionalized with graphene oxide, Desalin. Water Treat. 128 (2018) 20–26, https://doi.org/10.5004/dwt.2018.22570.

[32] H. Sun, B. Tang, P. Wu, Development of hybrid ultrafiltration membranes with improved water separation properties using modified superhydrophilic metal-organic framework nanoparticles, ACS Appl. Mater. Interfaces 9 (25) (2017) 21473–21484, https://doi.org/10.1021/acsami.7b05504.

[33] N.F. Razali, A.W. Mohammad, N. Hilal, C.P. Leo, J. Alam, Optimisation of polyethersulfone/polyaniline blended membranes using response surface methodology approach, Desalination 311 (2013) 182–191, https://doi.org/10.1016/j.desal.2012.11.033.

[34] J.L.C. Rowsell, O.M. Yaghi, Metal-organic frameworks: A new class of porous materials, Micropor. Mesopor. Mater. 73 (1-2) (2004) 3–14, https://doi.org/10.1016/j.micromeso.2004.03.034.

[35] H. Furukawa, U. Müller, O.M. Yaghi, "Heterogeneity within order" in metal-organic frameworks, Angew. Chem. Int. Edn 54 (11) (2015) 3417–3430, https://doi.org/10.1002/anie.201410252.

[36] S. Sorribas, P. Gorgojo, C. Téllez, J. Coronas, A.G. Livingston, High flux thin film nanocomposite membranes based on metal-organic frameworks for organic solvent nanofiltration, J. Am. Chem. Soc. 135 (40) (2013) 15201–15208, https://doi.org/10.1021/ja407665w.

[37] Z.X. Low, A. Razmjou, K. Wang, S. Gray, M. Duke, H. Wang, Effect of addition of two-dimensional ZIF-L nanoflakes on the properties of polyethersulfone ultrafiltration membrane, J. Membr. Sci. 460 (2014) 9–17, https://doi.org/10.1016/j.memsci.2014.02.026.

[38] Y. Li, L.H. Wee, A. Volodin, J.A. Martens, I.F.J. Vankelecom, Polymer supported ZIF-8 membranes prepared via an interfacial synthesis method, Chem. Commun. 51 (5) (2015) 918–920, https://doi.org/10.1039/c4cc06699e.

[39] S. Shahid, K. Nijmeijer, S. Nehache, I. Vankelecom, A. Deratani, D. Quemener, MOF-mixed matrix membranes: Precise dispersion of MOF particles with better compatibility via a particle fusion approach for enhanced gas separation properties, J. Membr. Sci. 492 (2015) 21–31, https://doi.org/10.1016/j.memsci.2015.05.015.

[40] H. Sun, B. Tang, P. Wu, Hydrophilic hollow zeolitic imidazolate framework-8 modified ultrafiltration membranes with significantly enhanced water separation properties, J. Membr. Sci. 551 (2018) 283–293, https://doi.org/10.1016/j.memsci.2018.01.053.

[41] F. Gholami, S. Zinadini, A.A. Zinatizadeh, A.R. Abbasi, TMU-5 metal-organic frameworks (MOFs) as a novel nanofiller for flux increment and fouling mitigation in PES ultrafiltration membrane, Sep. Purif. Technol. 194 (2018) 272–280, https://doi.org/10.1016/j.seppur.2017.11.054.

[42] B.-M. Jun, Y. Al-Hamadani, A. Son, C. Park, M. Jang, A. Jang, N. Kim, Y. Yoon, Applications of metal-organic framework based membranes in water purification: A review, Sep. Purif. Technol. 247 (2020) https://doi.org/10.1016/j.seppur.2020.116947.

[43] C. Klaysom, B.P. Ladewig, G.Q.M. Lu, L. Wang, Preparation and characterization of sulfonated polyethersulfone for cation-exchange membranes, J. Membr. Sci. 368 (1–2) (2011) 48–53, https://doi.org/10.1016/j.memsci.2010.11.006.

[44] S. Zinadini, A.A. Zinatizadeh, M. Rahimi, V. Vatanpour, Z. Rahimi, High power generation and COD removal in a microbial fuel cell operated by a novel sulfonated PES/PES blend proton exchange membrane, Energy 125 (2017) 427–438, https://doi.org/10.1016/j.energy.2017.02.146.

[45] P. Bai, X. Cao, Y. Zhang, Z. Yin, Q. Wei, C. Zhao, Modification of a polyethersulfone matrix by grafting functional groups and the research of biomedical performance, J. Biomater. Sci., Polym. Edn 21 (12) (2010) 1559–1572, https://doi.org/10.1163/092050609X12519805626158.

[46] J. Chen, K. Li, L. Chen, R. Liu, X. Huang, D. Ye, Conversion of fructose into 5-hydroxymethylfurfural catalyzed by recyclable sulfonic acid-functionalized metal-organic frameworks, Green Chem. 16 (5) (2014) 2490–2499, https://doi.org/10.1039/c3gc42414f.

[47] C. Hon Lau, R. Babarao, M.R. Hill, A route to drastic increase of CO2 uptake in Zr metal organic framework UiO-66, Chem. Commun. 49 (35) (2013) 3634–3636, https://doi.org/10.1039/c3cc40470f.

[48] M. Kim, J.F. Cahill, H. Fei, K.A. Prather, S.M. Cohen, Postsynthetic ligand and cation exchange in robust metal-organic frameworks, J. Am. Chem. Soc. 134 (43) (2012) 18082–18088, https://doi.org/10.1021/ja3079219.

[49] A. Schaate, P. Roy, A. Godt, J. Lippke, F. Waltz, M. Wiebcke, P. Behrens, Modulated synthesis of zr-based metal-organic frameworks: From nano to single crystals, Chemistry 17 (24) (2011) 6643–6651, https://doi.org/10.1002/chem.201003211.

[50] Y.C. Lin, H.H. Tseng, D.K. Wang, Uncovering the effects of PEG porogen molecular weight and concentration on ultrafiltration membrane properties and protein purification performance, J. Membr. Sci. 618 (September 2020) (2021) 118729, https://doi.org/10.1016/j.memsci.2020.118729, https://doi.org/10.1016/j.memsci.2020.118729.

[51] W. Ye, R. Liu, X. Chen, Q. Chen, J. Lin, X. Lin, B. Van der Bruggen, S. Zhao, Loose nanofiltration-based electrodialysis for highly efficient textile wastewater treatment, J. Membr. Sci. 608 (March) (2020) 118182, https://doi.org/10.1016/j.memsci.2020.118182, https://doi.org/10.1016/j.memsci.2020.118182.

[52] C. Tam, A. Tremblay, Membrane pore characterization-comparison between single and multicomponent solute probe techniques, J. Membr. Sci. 57 (2–3) (1991) 271–287, https://doi.org/10.1016/S0376-7388(00)80683-3.

[53] J.H. Cavka, S. Jakobsen, U. Olsbye, N. Guillou, C. Lamberti, S. Bordiga, K.P. Lillerud, A new zirconium inorganic building brick forming metal organic frameworks with exceptional stability, J. Am. Chem. Soc. 130 (42) (2008) 13850–13851, https://doi.org/10.1021/ja8057953.

[54] Y. Luan, Y. Qi, H. Gao, R.S. Andriamitantsoa, N. Zheng, G. Wang, A general post-synthetic modification approach of amino-tagged metal-organic frameworks to access efficient catalysts for the knoevenagel condensation reaction, J. Mater. Chem. A 3 (33) (2015) 17320–17331, https://doi.org/10.1039/c5ta00816f.

[55] S. Biswas, P. Van Der Voort, A general strategy for the synthesis of functionalised UiO-66 frameworks: Characterisation, stability and CO2 adsorption properties, Eur. J. Inorg. Chem. (12) (2013) 2154–2160, https://doi.org/10.1002/ejic.201201228.

[56] J. Ma, X. Guo, Y. Ying, D. Liu, C. Zhong, Composite ultrafiltration membrane tailored by MOF@GO with highly improved water purification performance, Chem. Eng. J. 313 (2017) 890–898, https://doi.org/10.1016/j.cej.2016.10.127.

[57] M. Kandiah, M.H. Nilsen, S. Usseglio, S. Jakobsen, U. Olsbye, M. Tilset, C. Larabi, E.A. Quadrelli, F. Bonino, K.P. Lillerud, Synthesis and stability of tagged UiO-66 Zr-MOFs, Chem. Mater. 22 (24) (2010) 6632–6640, https://doi.org/10.1021/cm102601v.

[58] J. Gascon, U. Aktay, M.D. Hernandez-Alonso, G.P.M. van Klink, F. Kapteijn, Amino-based metal-organic frameworks as stable, highly active basic catalysts, J. Catal. 261 (1) (2009) 75–87, https://doi.org/10.1016/j.jcat.2008.11.010.

[59] H. Jasuja, K.S. Walton, Experimental study of CO2, CH4, and water vapor adsorption on a dimethyl-functionalized UiO-66 framework, J. Phys. Chem. C 117 (14) (2013) 7062–7068, https://doi.org/10.1021/jp311857e.

[60] Y. Zhang, X. Feng, H. Li, Y. Chen, J. Zhao, S. Wang, L. Wang, B. Wang, Photoinduced postsynthetic polymerization of a metal-organic framework toward a flexible stand-alone membrane, Angew. Chem. Int. Edn 54 (14) (2015) 4259–4263, https://doi.org/10.1002/anie.201500207.

[61] L. Yu, Y. Zhang, B. Zhang, J. Liu, H. Zhang, C. Song, Preparation and characterization of HPEI-GO/PES ultrafiltration membrane with antifouling and antibacterial properties, J. Membr. Sci. 447 (2013) 452–462, https://doi.org/10.1016/j.memsci.2013.07.042.

[62] S. Zinadini, A.A. Zinatizadeh, M. Rahimi, V. Vatanpour, H. Zangeneh, Preparation of a novel antifouling mixed matrix PES membrane by embedding graphene oxide nanoplates, J. Membr. Sci. 453 (2014) 292–301, https://doi.org/10.1016/j.memsci.2013.10.070.

[63] A. Rahimpour, S.S. Madaeni, S. Ghorbani, A. Shockravi, Y. Mansourpanah, The influence of sulfonated polyethersulfone (SPES) on surface nano-morphology and performance of polyethersulfone (PES) membrane, Appl. Surf. Sci. 256 (6) (2010) 1825–1831, https://doi.org/10.1016/j.apsusc.2009.10.014.

[64] X. Liu, N.K. Demir, Z. Wu, K. Li, Highly water-stable zirconium metal-organic framework UiO-66 membranes supported on alumina hollow fibers for desalination, J. Am. Chem. Soc. 137 (22) (2015) 6999–7002, https://doi.org/10.1021/jacs.5b02276.

[65] D. Ma, S.B. Peh, G. Han, S.B. Chen, Thin-film nanocomposite (TFN) membranes incorporated with super-hydrophilic metal-organic framework (MOF) UiO-66: Toward enhancement of water flux and salt rejection, ACS Appl. Mater. Interfaces 9 (8) (2017) 7523–7534, https://doi.org/10.1021/acsami.6b14223.

[66] N. Wang, G. Zhang, L. Wang, J. Li, Q. An, S. Ji, Pervaporation dehydration of acetic acid using NH2-UiO-66/PEI mixed matrix membranes, Sep. Purif. Technol. 186 (2017) 20–27, https://doi.org/10.1016/j.seppur.2017.05.046.

[67] M. Golpour, M. Pakizeh, Preparation and characterization of new PA-MOF/PPSU-GO membrane for the separation of KHI from water, Chem. Eng. J. 345 (2018) 221–232, https://doi.org/10.1016/j.cej.2018.03.154.

[68] S. Jamshidifard, S. Koushkbaghi, S. Hosseini, S. Rezaei, A. Karamipour, A. Jafari rad, M. Irani, Incorporation of UiO-66-NH2 MOF into the PAN/chitosan nanofibers for adsorption and membrane filtration of Pb(II), Cd(II) and Cr(VI) ions from aqueous solutions, J. Hard Mater. 368 (2019) 10–20, https://doi.org/10.1016/j.jhazmat.2019.01.024.

[69] S. Li, Z. Cui, L. Zhang, B. He, J. Li, The effect of sulfonated polysulfone on the compatibility and structure of polyethersulfone-based blend membranes, J. Membr. Sci. 513 (2016) 1–11, https://doi.org/10.1016/j.memsci.2016.04.035.

[70] Z. Liu, Z. Mi, C. Chen, H. Zhou, X. Zhao, D. Wang, Preparation of hydrophilic and antifouling polysulfone ultrafiltration membrane derived from phenolphthalin by copolymerization method, Appl. Surf. Sci. 401 (2017) 69–78, https://doi.org/10.1016/j.apsusc.2016.12.228.

[71] A. Behboudi, Y. Jafarzadeh, R. Yegani, Polyvinyl chloride/polycarbonate blend ultrafiltration membranes for water treatment, J. Membr. Sci. 534 (2017) 18–24, https://doi.org/10.1016/j.memsci.2017.04.011.

[72] S. Zinadini, A.A. Zinatizadeh, M. Rahimi, V. Vatanpour, H. Zangeneh, M. Beygzadeh, Novel high flux antifouling nanofiltration membranes for dye removal containing carboxymethyl chitosan coated Fe3O4 nanoparticles, Desalination 349 (2014) 145–154, https://doi.org/10.1016/j.desal.2014.07.007.

[73] V. Vatanpour, S.S. Madaeni, R. Moradian, S. Zinadini, B. Astinchap, Novel antibifouling nanofiltration polyethersulfone membrane fabricated from embedding TiO2 coated multiwalled carbon nanotubes, Sep. Purif. Technol. 90 (2012) 69–82, https://doi.org/10.1016/j.seppur.2012.02.014.

[74] X. Chen, Y. Su, F. Shen, Y. Wan, Antifouling ultrafiltration membranes made from PAN-b-PEG copolymers: Effect of copolymer composition and PEG chain length, J. Membr. Sci. 384 (1–2) (2011) 44–51, https://doi.org/10.1016/j.memsci.2011.09.002.